Обзор Arxiv: astro-ph, 27 апреля - 9 мая 2018 года

От Сильченко О.К.

Astro-ph: 1805.02568

STAR FORMATION HISTORIES OF $Z \sim 1$ GALAXIES IN LEGA-C

Priscilla Chauke,[1] Arjen van der Wel,[2,1] Camilla Pacifici,[3] Rachel Bezanson,[4] Po-Feng Wu,[1] Anna Gallazzi,[5] Kai Noeske,[6] Caroline Straatman,[2] Juan-Carlos Muños-Mateos,[7] Marijn Franx,[8] Ivana Barišić,[9] Eric F. Bell,[10] Gabriel B. Brammer,[3] Joao Calhau,[11] Josha van Houdt,[9] Ivo Labbé,[8] Michael V. Maseda,[8] Adam Muzzin,[12] Hans-Walter Rix,[9] and David Sobral[8,11]

[1] Max-Planck-Institut für Astronomie, Königstuhl 17, D-69117 Heidelberg, Germany
[2] Sterrenkundig Observatorium, Universiteit Gent, Krijgslaan 281 S9, B-9000 Gent, Belgium
[3] Space Telescope Science Institute, 3700 San Martin Drive, Baltimore, MD 21218, USA
[4] University of Pittsburgh, Department of Physics and Astronomy, 100 Allen Hall, 3941 O'Hara St, Pittsburgh PA 15260, USA
[5] INAF-Osservatorio Astrofisico di Arcetri, Largo Enrico, Fermi 5, I-50125 Firenze, Italy
[6] Experimenta Heilbronn, Kranenstraße 14, 74072, Heilbronn, Germany
[7] European Southern Observatory, Alonso de Cordova 3107, Casilla 19001, Vitacura, Santiago, Chile
[8] Leiden Observatory, Leiden University, PO Box 9513, 2300 RA Leiden, The Netherlands
[9] Max-Planck Institut für Astronomie, Königstuhl 17, D-69117, Heidelberg, Germany
[10] Department of Astronomy, University of Michigan, 1085 S. University Ave., Ann Arbor, MI 48109, USA
[11] Physics Department, Lancaster University, Lancaster LA1 4YB, UK
[12] Department of Physics and Astronomy, York University, 4700 Keele St., Toronto, Ontario, MJ3 1P3, Canada

Обзор LEGA-C

2. DATA

LEGA-C (van der Wel et al. 2016) is an ongoing ESO Public Spectroscopic survey with VLT/VIMOS of ~ 3000 galaxies in the COSMOS field ($R.A. = 10^h00^m$; $Dec. = +2°12'$). The galaxies were selected from the Ultra-VISTA catalog (Muzzin et al. 2013b), with redshifts in the range $0.6 < z < 1.0$. The galaxies were K-band selected with a magnitude limit ranging from $K(AB) = 21.08$ at z = 0.6 to $K(AB) = 20.7$ at z = 0.8 to $K(AB) = 20.36$ at z = 1.0 (stellar masses $M_* > 10^{10} M_\odot$). These criteria were chosen to reduce the dependence on variations in age, SF activity and extinction, as well as ensure that the targets were bright enough in the observed wavelength range ($0.6\mu m - 0.9\mu m$) to obtain high quality, high resolution spectra (R ~ 3000). Each galaxy is observed for ~ 20 h, which results in spectra with $S/N \sim 20\,\text{Å}^{-1}$.

The analyses in this work are based on the first-year data release[1], which contains spectra of 892 galaxies, 678 of which are in the primary sample and have a $S/N > 5\,\text{Å}^{-1}$ between rest-frame wavelengths $4000\,\text{Å}$ and $4300\,\text{Å}$ (typically, $S/N \sim 20\,\text{Å}^{-1}$). Emission line subtracted spectra are used in the fitting algorithm;

Восстановление историй звездообразования☺

Table 1. Properties of the *FSPS* template spectra.

Age Bin[a]	SFR[b]	M$_*$[c]	L$_{bol}$[d]
log(yr)	M$_\odot$/yr	M$_\odot$	log(L$_\odot$)
$0.000 - 8.000$	1.000×10^{-8}	0.837	1.964
$8.000 - 8.300$	1.005×10^{-8}	0.711	0.885
$8.300 - 8.475$	1.010×10^{-8}	0.748	0.650
$8.475 - 8.650$	6.750×10^{-9}	0.731	0.497
$8.650 - 8.750$	8.646×10^{-9}	0.718	0.382
$8.750 - 8.875$	5.332×10^{-9}	0.707	0.285
$8.875 - 9.000$	3.998×10^{-9}	0.695	0.187
$9.000 - 9.075$	5.305×10^{-9}	0.685	0.127
$9.075 - 9.225$	2.040×10^{-9}	0.671	0.099
$9.225 - 9.375$	1.444×10^{-9}	0.652	-0.043
$9.375 - 9.525$	1.022×10^{-9}	0.639	-0.161
$9.525 - 9.845$	2.681×10^{-10}	0.618	-0.347

[a] Age interval of CSP templates.

[b] SFR s.t. $1\,M_\odot$ of stars formed within the interval.

[c] Stellar mass (including stellar remnants) with mass loss accounted for.
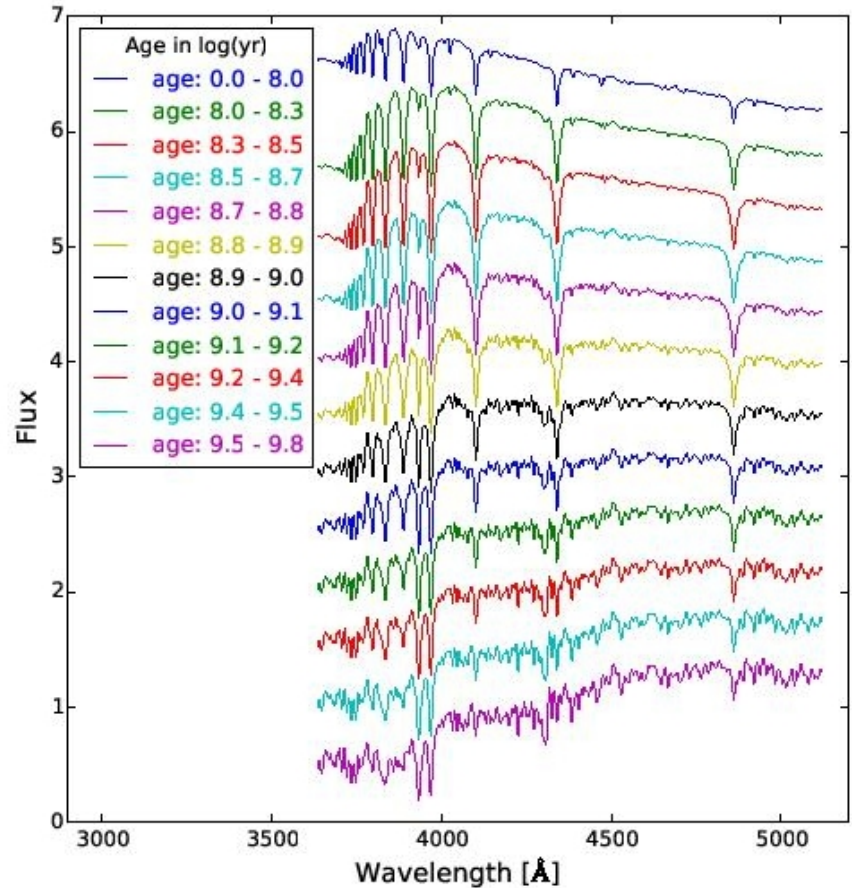
[d] Bolometric luminosity.

Figure 1. Template CSP spectra used to fit LEGA-C galaxies. They were generated from *FSPS*, using the time intervals listed in Table 1, with solar metallicity and arbitrary velocity dispersion; and they have been normalised and shifted here

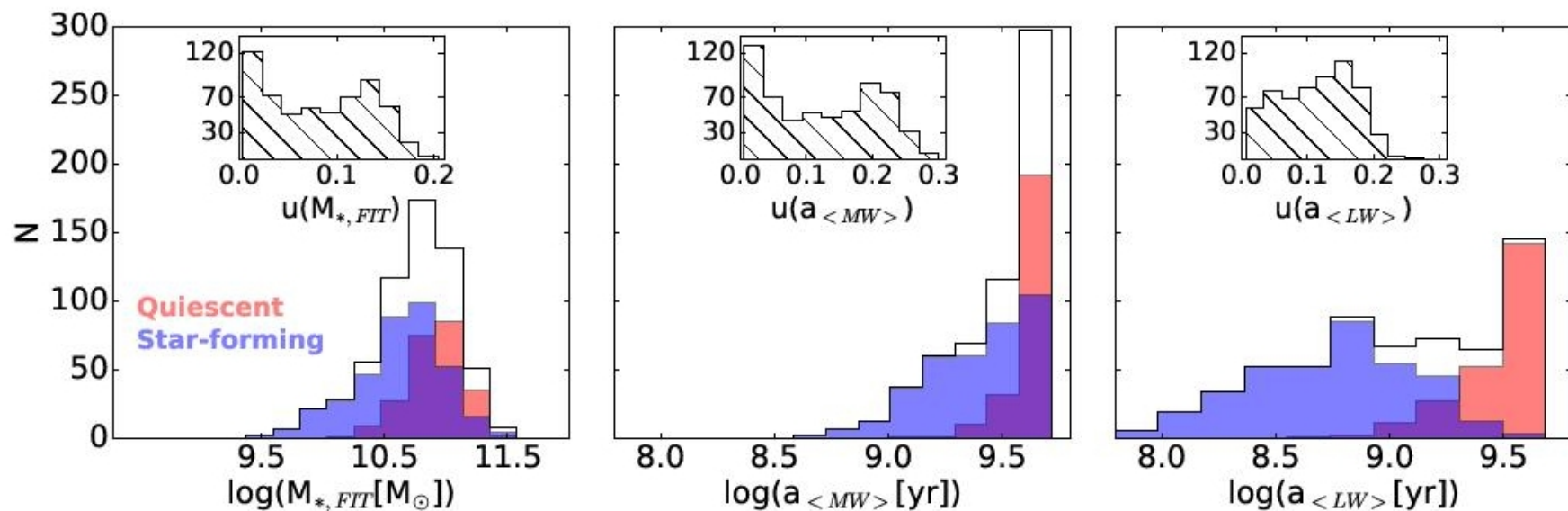# Галактики с текущим звездообразованием и без оного

Figure 3. Distributions of $M_{*,FIT}$ (left), $a_{<MW>}$ (middle) and $a_{<LW>}$ (right) of the LEGA-C sample. The quiescent and star-forming populations (as defined in Section 5.1) are shown in red and blue, respectively. The distribution of the uncertainties for each parameter are shown at the top of each figure.
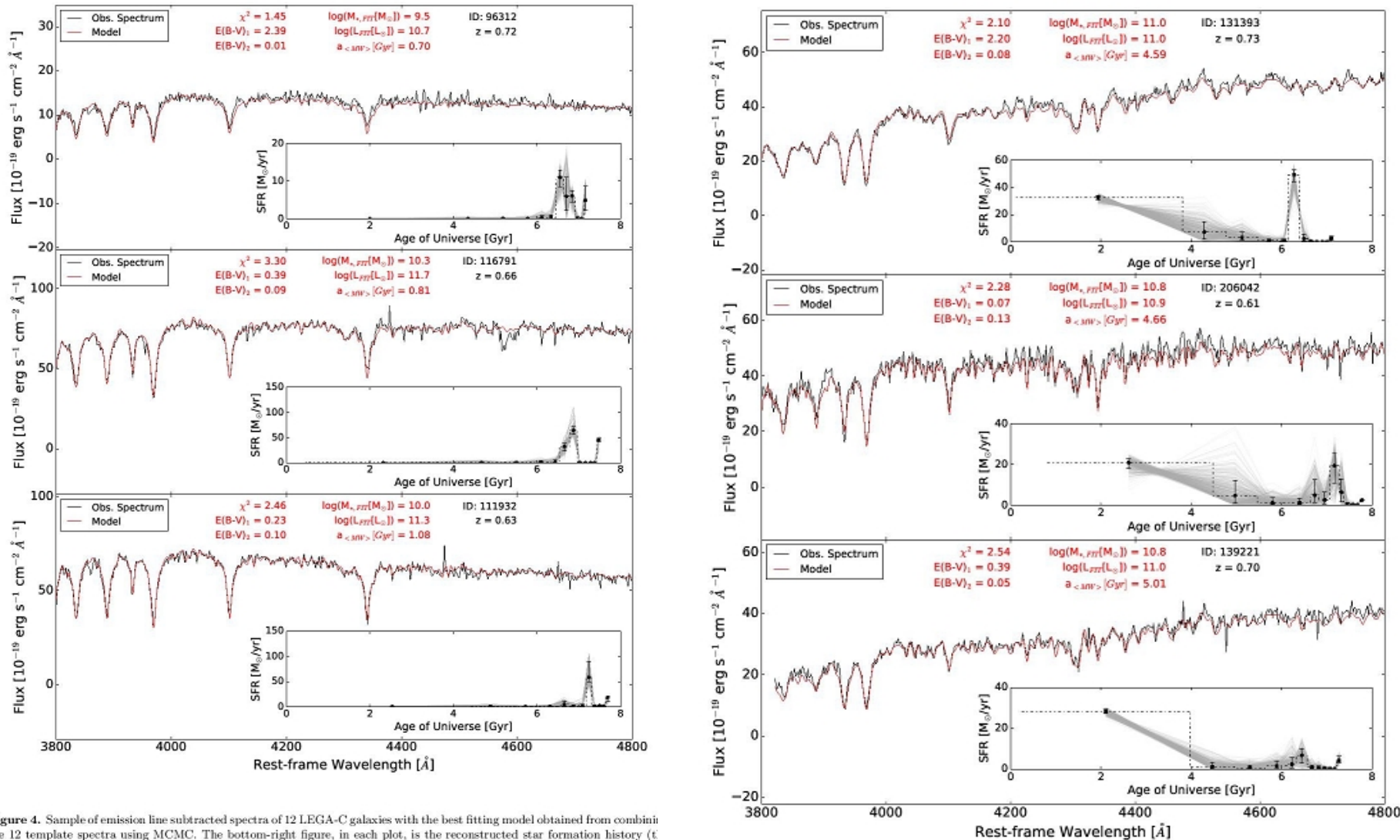
Примеры спектров и историй SF

Figure 4. Sample of emission line subtracted spectra of 12 LEGA-C galaxies with the best fitting model obtained from combini... the 12 template spectra using MCMC. The bottom-right figure, in each plot, is the reconstructed star formation history (t... converged walkers are shown in grey). The MCMC resultant mass, luminosity, mass-weighted age and dust reddening valu... are shown in red. The spectra are ordered by $a_{<MW>}$.
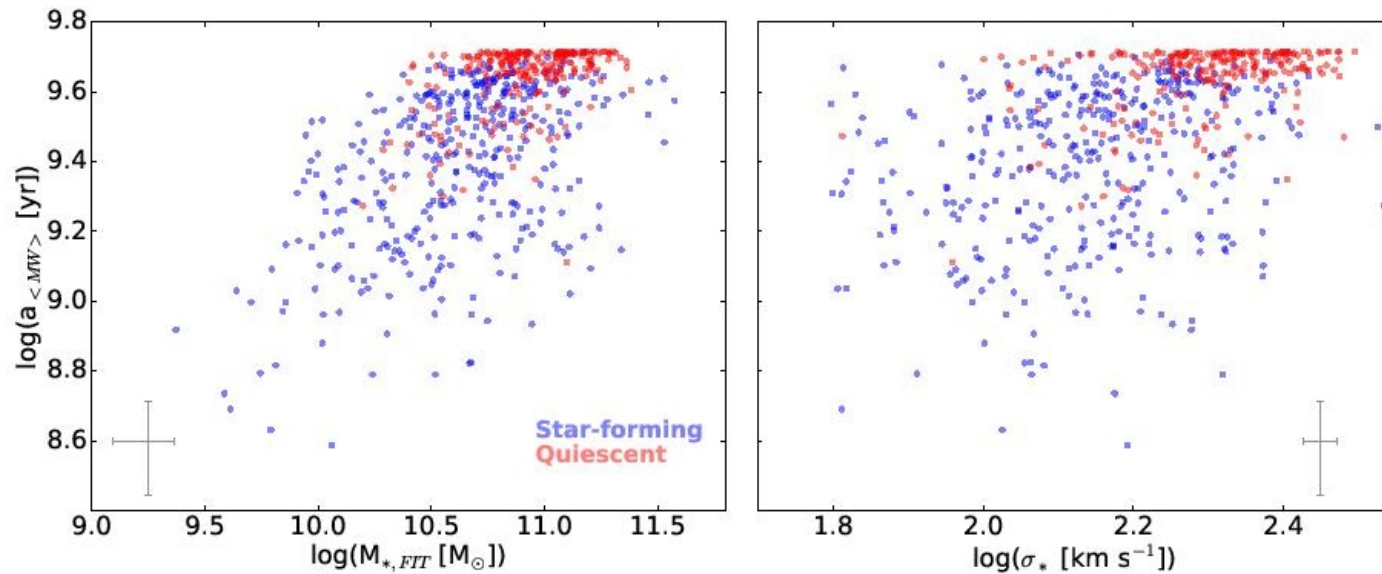
Всякие корреляции

Figure 6. $a_{<MW>}$ as a function of $M_{*,FIT}$ (left) and σ_* (right). The star-forming and quiescent populations are indicated in blue and red, respectively, and typical error bars are indicated in grey. Galaxies with $\sigma_* \gtrsim 200\,\mathrm{km\,s^{-1}}$ are almost exclusively old ($> 4\mathrm{Gyrs}$) and quiescent, which indicates that σ_* is a stronger predictor of age and SF activity.
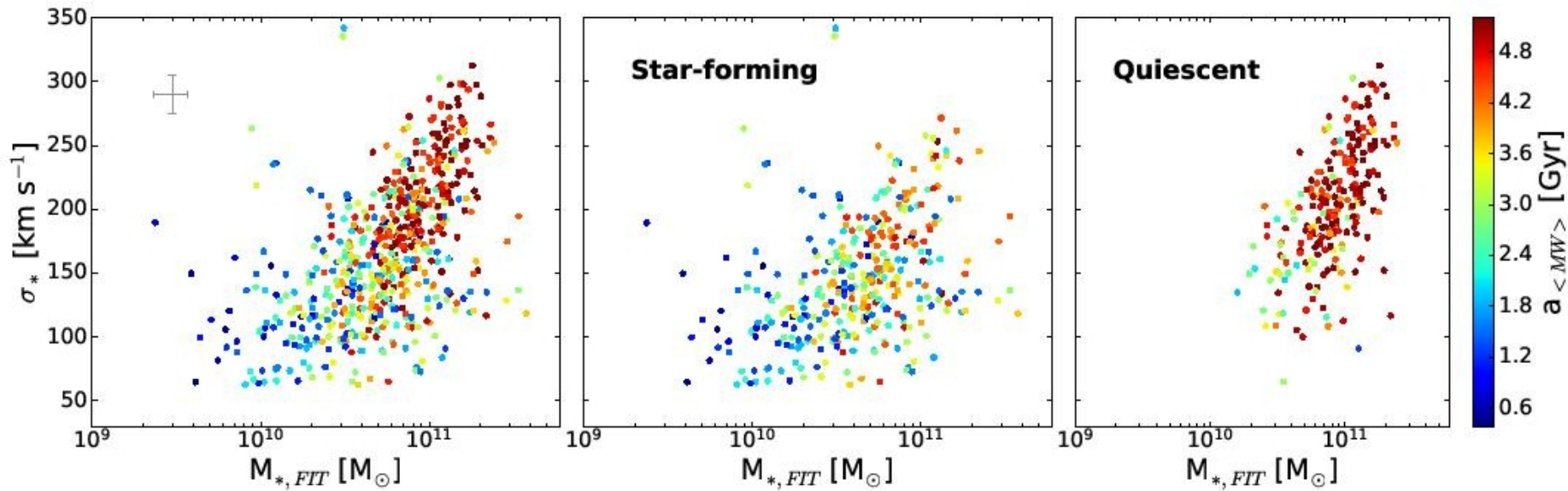
Всякие корреляции

Figure 7. σ_* versus $M_{*,FIT}$, colour-coded by $a_{<MW>}$. The star-forming and quiescent populations are shown in the middle and right panels, respectively. Typical error bars are indicated in grey. The clear separation between young and old galaxies at $\sigma_* \sim 170\,\mathrm{km\,s^{-1}}$ shows a stronger correlation between $a_{<MW>}$ and σ_* over $M_{*,FIT}$, which also depends on the current SF activity.
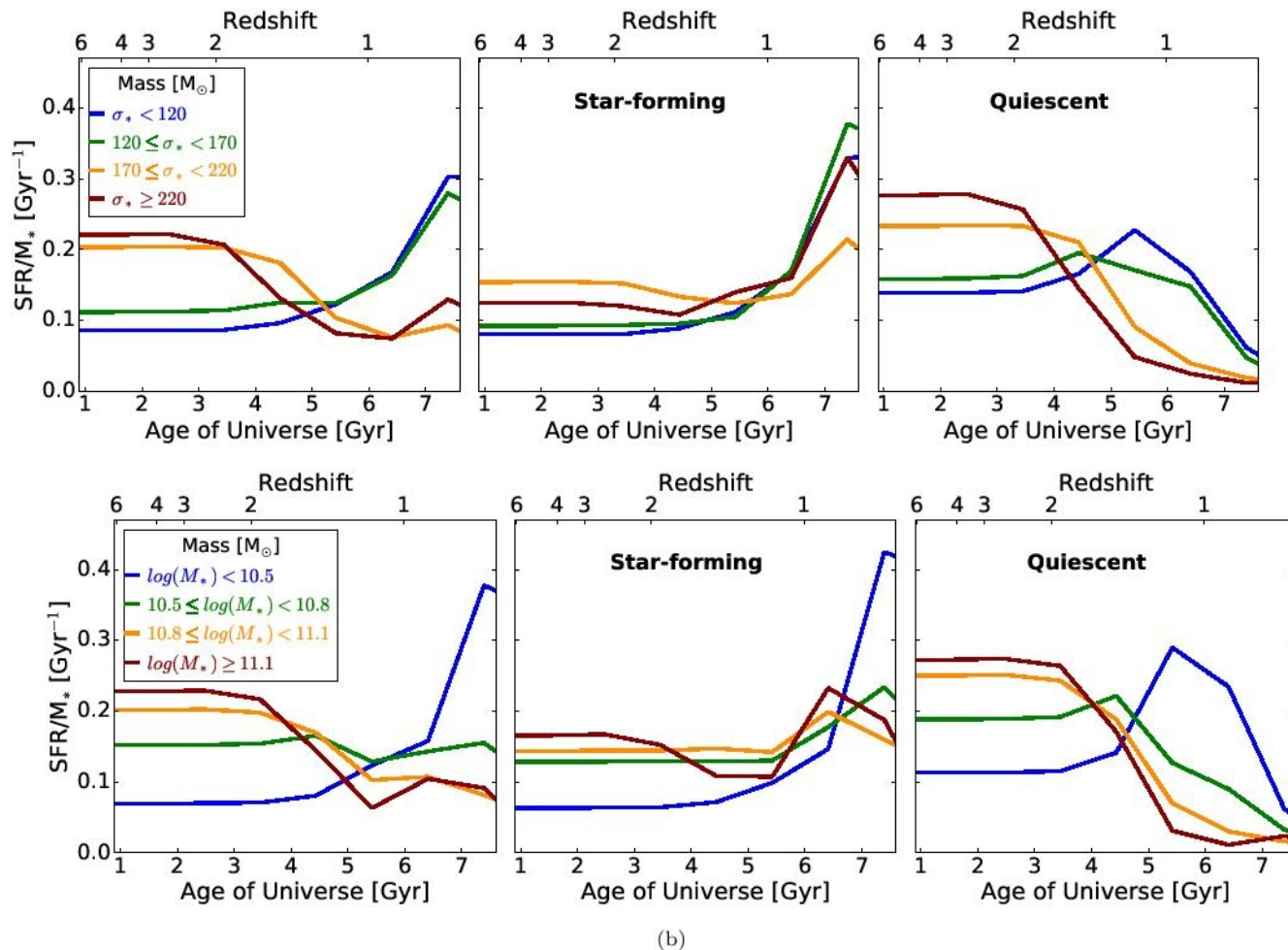
Типичные истории SF в бинах по массам

Figure 8. Ensemble-averaged SFHs of LEGA-C galaxies, normalised by stellar mass and separated into various σ_* (top) and $M_{*,FIT}$, bins (bottom). The histories are divided into the star-forming and quiescent populations in the middle and right panels, respectively. The stellar content in massive galaxies formed earlier and faster, regardless of current SF activity.

Astro-ph: 1805.02667

MOLECULAR GAS CONTENTS AND SCALING RELATIONS FOR MASSIVE PASSIVE GALAXIES AT INTERMEDIATE REDSHIFTS FROM THE LEGA-C SURVEY

Justin Spilker,[1] Rachel Bezanson,[2] Ivana Barišić,[3] Eric Bell,[4] Claudia del P. Lagos,[5,6] Michael Maseda,[7] Adam Muzzin,[8] Camilla Pacifici,[9,10] David Sobral,[11] Caroline Straatman,[12] Arjen van der Wel,[12,3] Pieter van Dokkum,[13] Benjamin Weiner,[14] Katherine Whitaker,[15] Christina C. Williams,[14,*] and Po-Feng Wu[3]

[1] Department of Astronomy, University of Texas at Austin, 2515 Speedway, Stop C1400, Austin, TX 78712, USA

[2] Department of Physics and Astronomy and PITT PACC, University of Pittsburgh, Pittsburgh, PA 15260, USA

[3] Max-Planck-Institut für Astronomie, Königstuhl 17, D-69117, Heidelberg, Germany

[4] Department of Astronomy, University of Michigan, 1085 South University Avenue, Ann Arbor, MI 48109-1107, USA

[5] International Centre for Radio Astronomy Research, M468, University of Western Australia, 35 Stirling Hwy, Crawley, WA 6009, Australia

[6] ARC Centre of Excellence for All Sky Astrophysics in 3 Dimensions (ASTRO 3D), 44 Rosehill Street Redfern, NSW 2016, Australia

[7] Leiden Observatory, Leiden University, PO Box 9513, 2300 RA Leiden, The Netherlands

[8] Department of Physics and Astronomy, York University, 4700 Keele St., Toronto, Ontario, M3J 1P3, Canada

[9] Astrophysics Science Division, Goddard Space Flight Center, Code 665, Greenbelt, MD 20771, USA

[10] Space Telescope Science Institute, 3700 San Martin Drive, Baltimore, MD 21218, USA

[11] Physics Department, Lancaster University, Lancaster LA1 4YB, UK

[12] Sterrenkundig Observatorium, Universiteit Gent, Krijgslaan 281 S9, B-9000 Gent, Belgium

[13] Astronomy Department, Yale University, New Haven, CT 06511, USA

[14] Steward Observatory, University of Arizona, 933 North Cherry Ave., Tucson, AZ 85721, USA

[15] Department of Physics, University of Connecticut, 2152 Hillside Road, Unit 3046, Storrs, CT 06269, USA

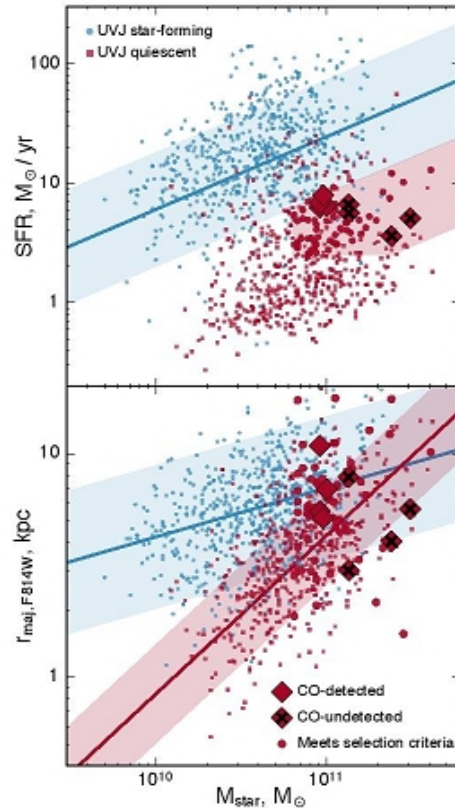# Все 8 объектов, предназначенных на ALMA
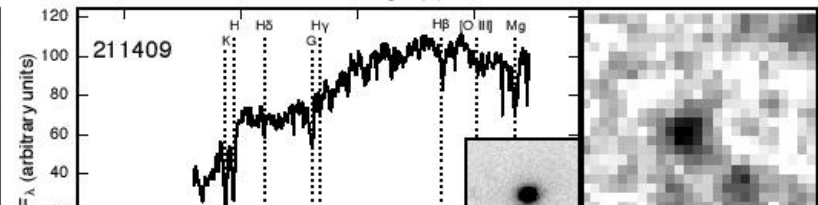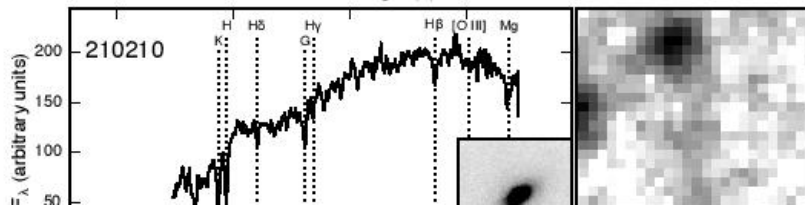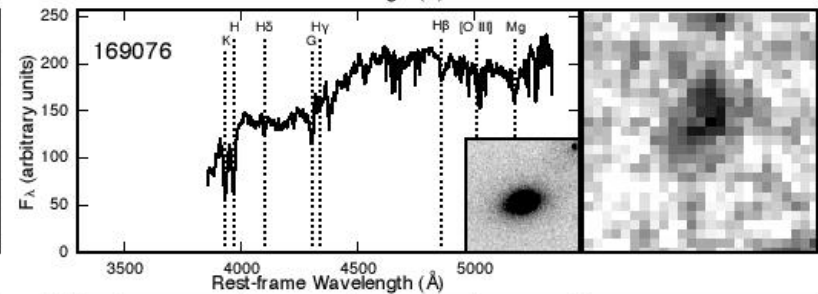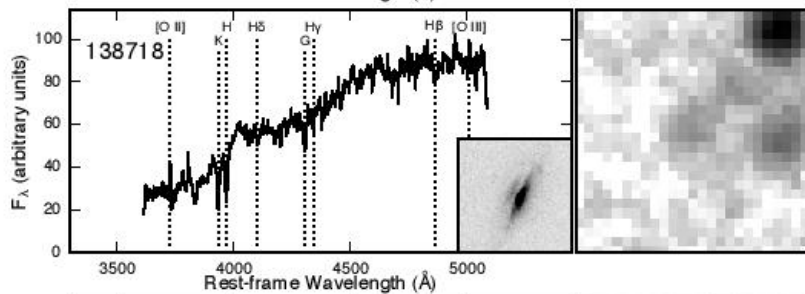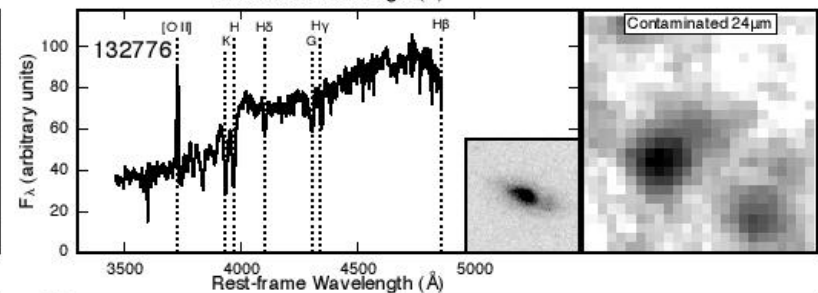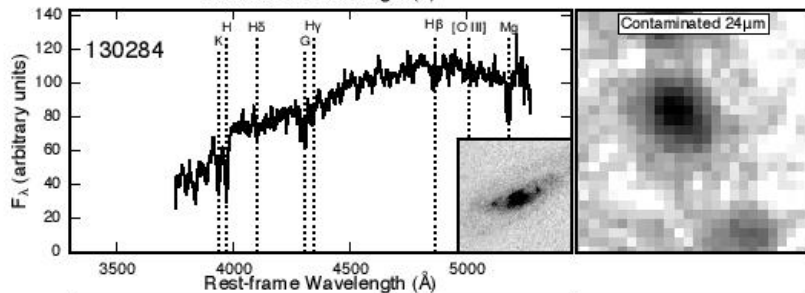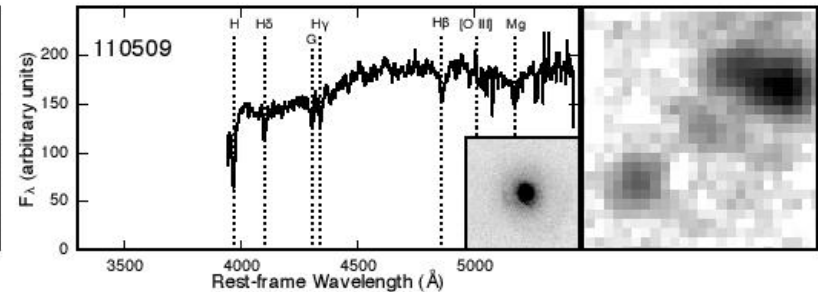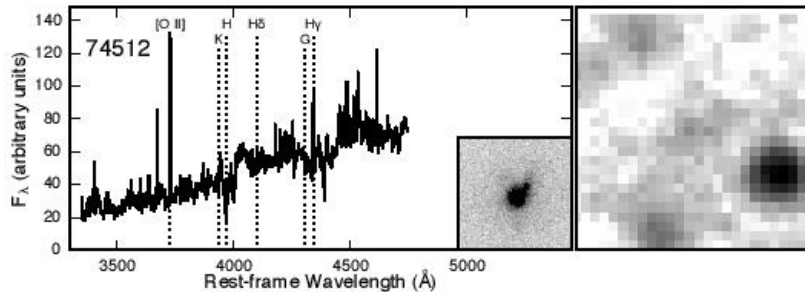
Их свойства

Figure 2. The selection of the ALMA-observed massive, passive sample with respect to the full LEGA-C sample. In both panels, the LEGA-C sample galaxies are color-coded blue (red) if they are classified as star-forming (quiescent) in rest-frame UVJ space (see Figure 3). Red circles are all LEGA-C galaxies that meet our selection criteria, while the ALMA-observed objects are shown with large red diamonds; CO-undetected objects are also marked with a black '×'. *Top:* The ALMA sample was primarily selected based on stellar mass and SFR; see text for details. The blue line shows the star-forming sequence at $z = 0.7$ from Whitaker et al. (2012), and the blue shaded region encompasses SFRs a factor of 3 above and below the relation. The red shaded region shows our selection box of massive and passive galaxies. *Bottom:* Size-mass relation for the LEGA-C and ALMA samples. Blue and red lines and regions show the size-mass relations for star-forming and quiescent galaxies at $z = 0.75$ from van der Wel et al. (2014).
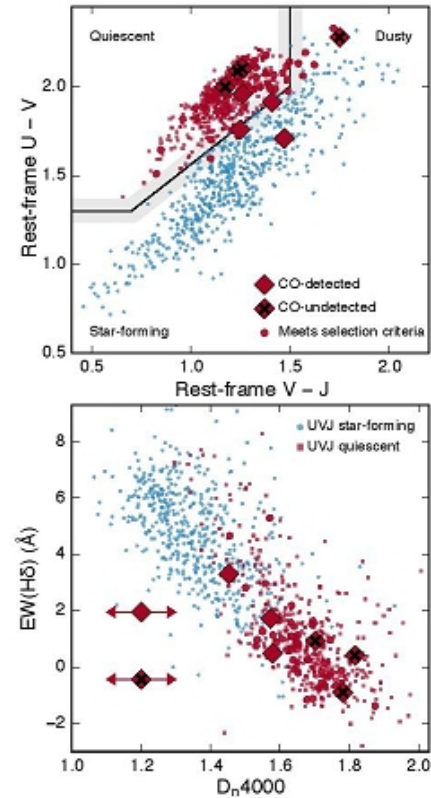
Figure 3. Symbols are plotted as in Figure 2. *Top:* Rest-frame UVJ color-color diagram for the LEGA-C galaxies and the ALMA sample, with the division between star-forming and quiescent galaxies of Muzzin et al. (2013) shown with the black line. The gray shaded band around this line represents both the differences in divisions found in the literature and an expectation that galaxies must transition from one region to the other over a period of time. Although this diagram was not used in the selection of the ALMA sample, six of the eight targets lie within (given the uncertainties) the quiescent region of the diagram at upper left. *Bottom:* The D_n4000 index against the $H\delta$ equivalent width, a proxy for the age of the stellar populations, with older and more massive systems located towards the lower right. We infer typical stellar ages of 1–3 Gyr for the ALMA sample; these objects are not recently quenched. For two objects (IDs 110509 and 169076), the LEGA-C spectra do not extend sufficiently blueward to measure D_n4000, shown arbitrarily at $D_n4000 = 1.2$ with arrows in each direction.

Результаты

Table 1. ALMA-Observed LEGA-C Sample Target Properties

LEGA-C ID	Right Ascension	Declination	$z_{\rm spec}$	$\log M_{\rm star}/M_\odot$	SFR	$\sigma^a_{100\,\rm km\,s^{-1}}$	$S_{\rm CO(2-1)}\Delta v$	$\log M_{\rm H_2}/M_\odot$
—	—	—	—	—	$M_\odot$/yr	μJy/beam	Jy km s^{-1}	—
74512	$10^{\rm h}01^{\rm m}42.88^{\rm s}$	$+02°01'21.9''$	0.7330	10.96	6.3	132	0.16 ± 0.04	9.82 ± 0.13
110509	$10^{\rm h}01^{\rm m}04.44^{\rm s}$	$+02°04'37.2''$	0.6671	11.00	6.5	160	0.24 ± 0.04	9.92 ± 0.07
130284	$10^{\rm h}00^{\rm m}13.78^{\rm s}$	$+02°19'37.0''$	0.6017	10.96	6.8	151	0.36 ± 0.04	10.00 ± 0.06
132776	$10^{\rm h}00^{\rm m}12.43^{\rm s}$	$+02°21'21.9''$	0.7500	10.98	7.9	163	0.33 ± 0.07	10.16 ± 0.11
138718	$10^{\rm h}00^{\rm m}13.89^{\rm s}$	$+02°25'38.0''$	0.6558	11.13	5.6	188	<0.21	<9.84
169076	$09^{\rm h}59^{\rm m}07.30^{\rm s}$	$+02°19'05.8''$	0.6772	11.49	5.1	256	<0.23	<9.91
210210	$10^{\rm h}00^{\rm m}35.55^{\rm s}$	$+02°31'04.2''$	0.6544	11.38	3.6	212	<0.21	<9.84
211409	$10^{\rm h}01^{\rm m}05.45^{\rm s}$	$+02°32'03.7''$	0.7140	11.13	6.6	188	<0.13	<9.72
Stacked Non-detections			0.6754	11.31	5.3	106	<0.093	<9.51

^{a} ALMA rms sensitivity in $100\,\rm km\,s^{-1}$ channels, naturally-weighted images

NOTE—LEGA-C ID numbers are the same as in the UltraVISTA catalog of Muzzin et al. (2013). Stellar masses are determined by fitting to multiwavelength photometry using FAST. SFRs are based on a weighted sum of UV and IR ($24\,\mu$m) fluxes. Integrated CO(2–1) line fluxes are converted to molecular gas masses under the assumptions described in Section 2.3. Upper limits for non-detections are 3σ, and molecular gas masses can be rescaled under different assumptions as $M_{\rm H_2}(0.8/r_{21})(\alpha_{\rm CO}/4.4)$.
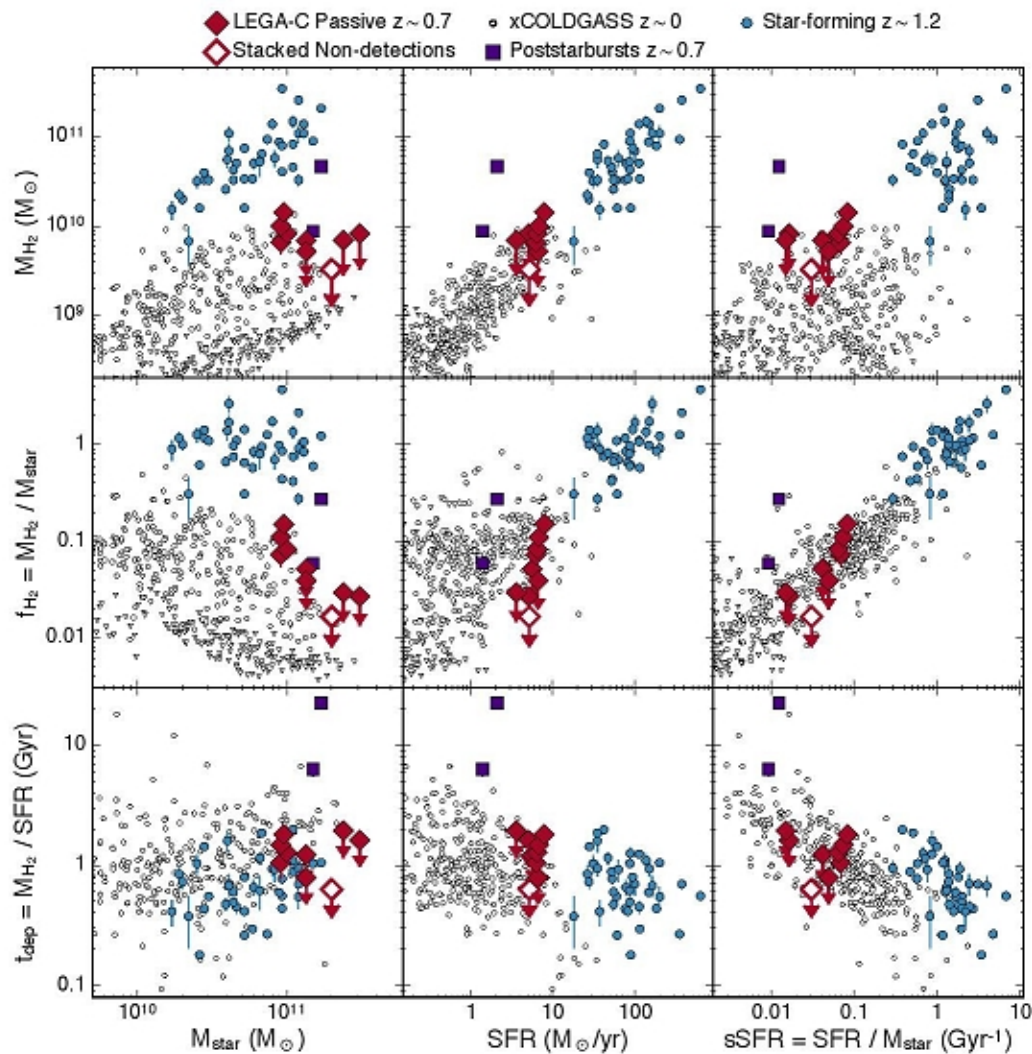
Результаты

Figure 5. Summary of basic results derived from our data, with comparison samples detailed in the text. From top to bottom, each row plots the molecular gas mass M_{H_2}, gas fraction f_{H_2}, and gas depletion time t_{dep}; from left to right each column shows the stellar mass M_{star}, star formation rate SFR, and specific SFR. The comparison samples are drawn from Tacconi et al. (2013); Papovich et al. (2016); Saintonge et al. (2017); Suess et al. (2017). All upper limits are 3σ. For clarity of presentation, we do not show upper limits for the xCOLDGASS sample in the bottom (t_{dep}) row.

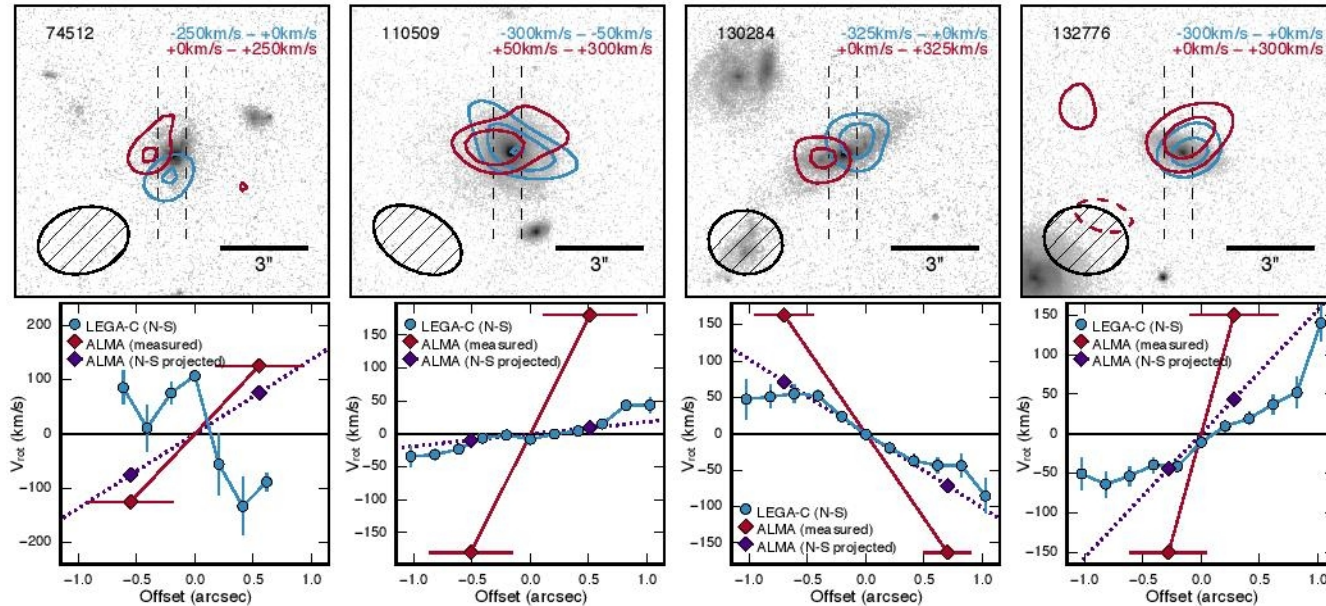# Грубо – вращение молекулярного газа; вроде лежит в плоскости

Figure 6. *Top:* Channel maps for each of the targets detected in CO(2–1) emission. The background grayscale shows the *HST*/ACS F814W image of each source, logarithmically scaled. Vertical dashed lines indicate the width and orientation of the LEGA-C VIMOS slits. For each target, we re-image the CO emission in two velocity bins that roughly equally split the total line emission, using the velocity ranges indicated for each source. The blue and red contours show the blue and red velocity components of the CO line in steps of 1σ beginning at $\pm 3\sigma$. The ALMA synthesized beam is shown with an ellipse at lower left; north is up and east is left. We note that the centroid of each component can be determined to less than a synthesized beam width. Significant velocity gradients are observed in three of four sources; given the modest signal-to-noise, the centroids of the blue and red components of ID 132776 are indistinguishable. *Bottom:* CO(2–1) rotation curves derived from the data

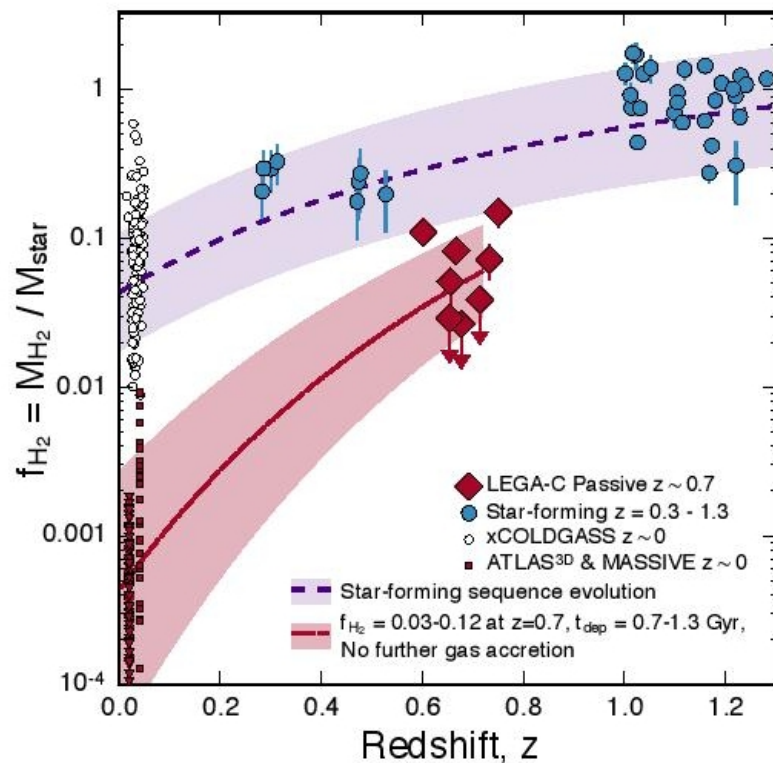# Спекуляции по поводу эволюции: не случилось аккреции?

Figure 9. Evolution of f_{H_2} with redshift for galaxies on and below the star-forming sequence. Our observations are shown with red diamonds, blue circles show galaxies near the star-forming sequence at $0.3 < z < 1.3$ (Bauermeister et al. 2013; Tacconi et al. 2013), white circles are $z < 0.05$ star-forming galaxies with $10 < \log M_{star}/M_\odot < 10.7$ from xCOLDGASS (Saintonge et al. 2017), and small red symbols

Stellar and Molecular Gas Rotation in a Recently-Quenched Massive Galaxy at z ~ 0.7

Qiana Hunt,[1] Rachel Bezanson,[2] Jenny E. Greene,[1] Justin S. Spilker,[3] Katherine A. Suess,[4] Mariska Kriek,[4] Desika Narayanan,[5, 6, 7] Robert Feldmann,[8] Arjen van der Wel,[9, 10] and Petchara Pattarakijwanich[11]

[1] Department of Astrophysics, Princeton University, Princeton, NJ 08544, USA

[2] Department of Physics and Astronomy and PITT PACC, University of Pittsburgh, Pittsburgh, PA, 15260, USA

[3] Department of Astronomy, University of Texas at Austin, 2515 Speedway, Stop C1400, Austin, TX 78712, USA

[4] Astronomy Department, University of California, Berkeley, CA 94720, USA

[5] Department of Astronomy, University of Florida, 211 Bryant Space Sciences Center, Gainesville, FL 32611, USA

[6] University of Florida Informatics Institute, 432 Newell Drive, Gainesville, FL 32511, USA

[7] Cosmic Dawn Center (DAWN), Niels Bohr Institute, University of Copenhagen, Juliane Maries vej 30, DK-2100 Copenhagen, Denmark

[8] Institute for Computational Science, University of Zurich, CH-8057 Zurich, Switzerland

[9] Sterrenkundig Observatorium, Universiteit Gent, Krijgslaan 281 S9, B-9000 Gent, Belgium

[10] Max-Planck Institut für Astronomie, Königstuhl 17, D-69117, Heidelberg, Germany

[11] Department of Physics, Faculty of Science, Mahidol University, Bangkok 10400, Thailand

ABSTRACT

The process by which massive galaxies transition from blue, star-forming disks into red, quiescent galaxies remains one of the most poorly-understood aspects of galaxy evolution. In this investigation, we attempt to gain a better understanding of how star formation is quenched by focusing on a massive post-starburst galaxy at z = 0.747. The target has a high stellar mass and a molecular gas fraction of 30% — unusually high for its low star formation rate. We look for indicators of star formation suppression mechanisms in the stellar kinematics and age distribution of the galaxy obtained from spatially resolved Gemini Integral-Field spectra and in the gas kinematics obtained from ALMA. We find evidence of significant rotation in the stars, but we do not detect a stellar age gradient within 5 kpc. The molecular gas is aligned with the stellar component, and we see no evidence of strong gas outflows. Our target may represent the product of a merger-induced starburst or of morphological quenching; however, our results are not completely consistent with any of the prominent quenching models.

Про галактику

In this Letter, we examine an intermediate-redshift PSB, SDSS J0912+1523, with a stellar mass of $\sim 2\times10^{11}$ M$_\odot$. The target was chosen out of a large sample of PSBs (Suess et al. 2017) selected from the SDSS DR12 catalog (Alam et al. 2015) and included in Pattarakijwanich et al. (2016). The galaxies in the PSB sample were identified by their strong Balmer breaks and blue slopes redward of the break, as demonstrated in Kriek et al. (2010). SDSS J0912+1523 was chosen as the brightest, most A-star dominated source at the high end of the sample's redshift range, with z = 0.747 and i_{AB} = 18.6 mag. SDSS J0912+1523 represents a rare opportunity to study the spatially resolved kinematics of a massive, recently-quenched PSB. Suess et al. (2017) present ALMA observations of the galaxy's molecular gas. Here, we analyze the stellar component observed by Gemini to obtain the kinematic properties and age distribution of the stellar population. Combining the stellar and gas data, we identify markers left by the quenching process and constrain the means by which SDSS J0912+1523 suppressed its star formation. We assume a cosmology of $\Omega_m = 0.3$, $\Omega_\Lambda = 0.7$, and $h = 0.7$.

Так выглядит она и ее спектр
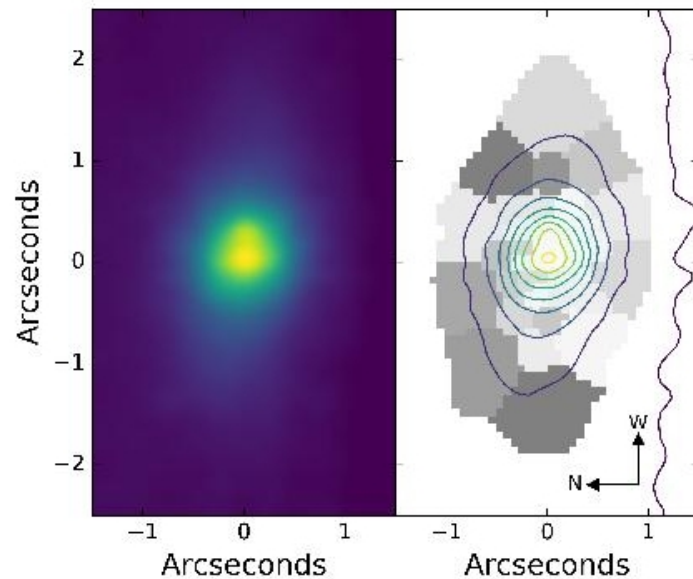
(a) Flux density of SDSS J0912+1523
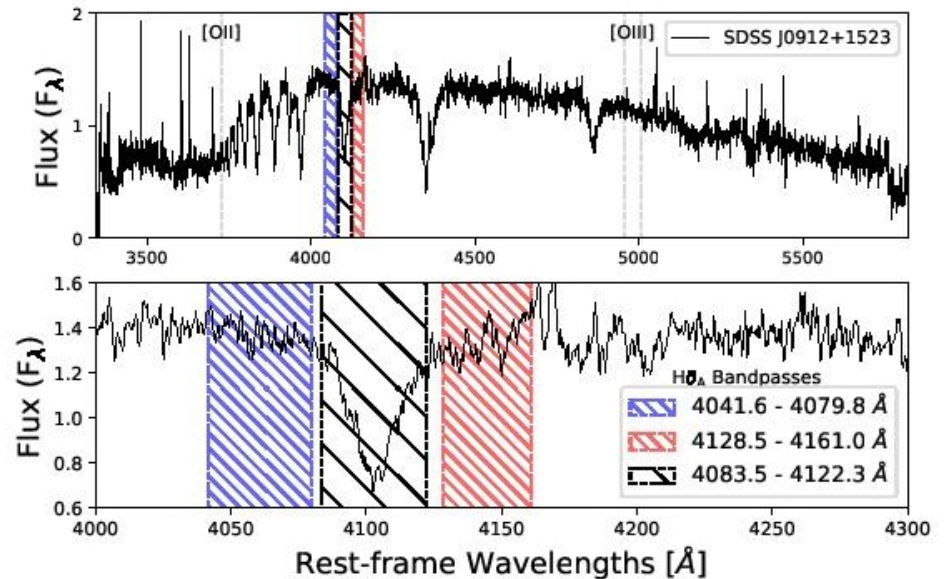
(b) Central spectrum and Hδ_A bandpasses

Figure 1. (a) Median flux map of SDSS J0912+1523 from the Gemini spectra, with contours overlaid onto the Voronoi bins. (b) Full spectrum of the central Voronoi bin and the Hδ_A central bandpass, surrounded by blue and red 'continuum' bandpasses, as defined by Worthey & Ottaviani (1997). The wavelengths of the [OII]λ3727, [OIII]λ4959, and [OIII]λ5007 lines are labeled.

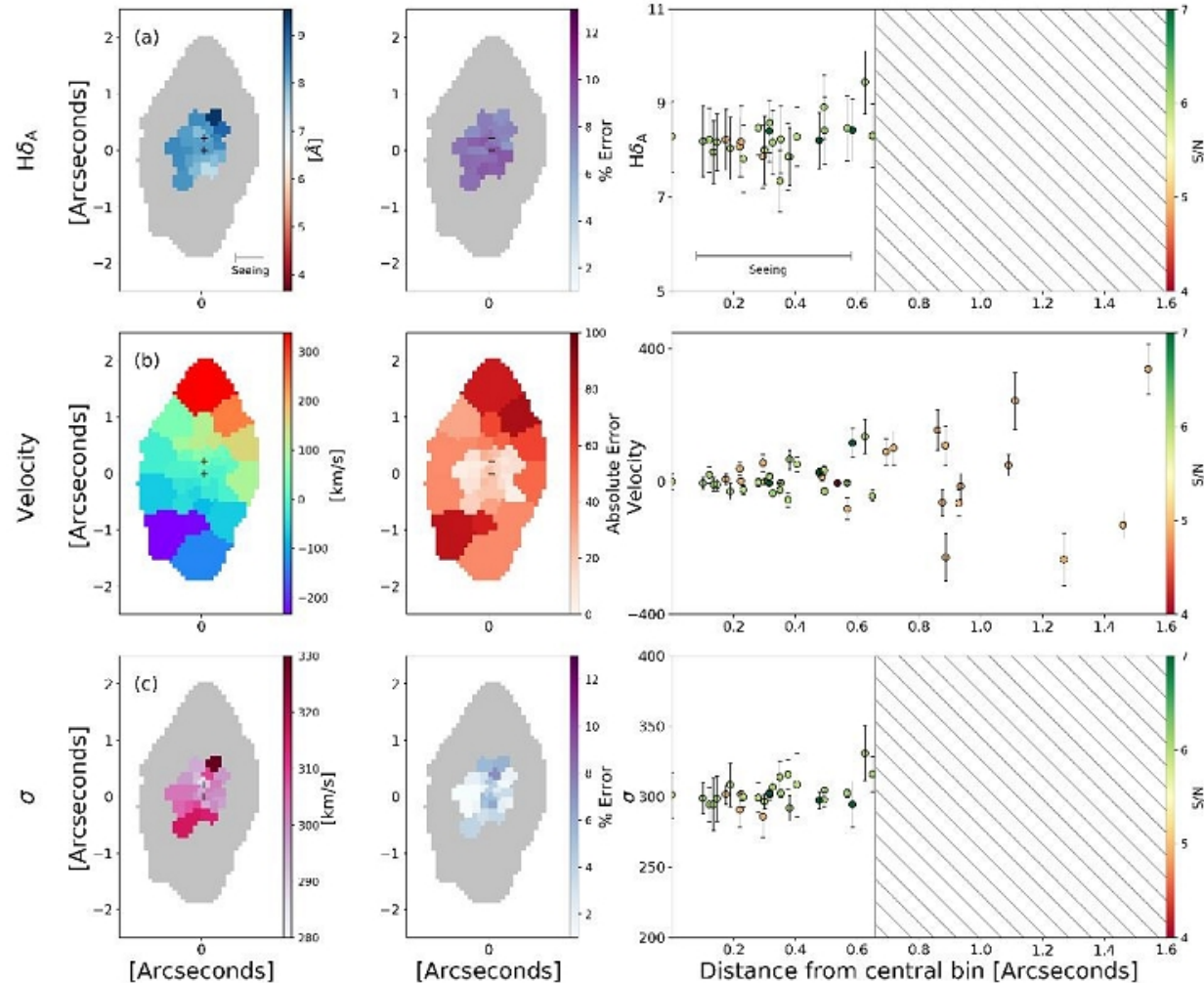# Результаты: никаких градиентов?

Figure 2. Stellar kinematic and spectral index maps. The two flux peaks are marked with black + symbols. The seeing is indicated with grey bars. The left column shows the measured values of the (a) equivalent width of Hδ_A, (b) velocity, and (c) velocity dispersion σ for each Voronoi bin. The middle column represents the estimated errors for each measurement. Velocity (row b) is measured with respect to the central bin, and its errors are presented as absolute values. The right column illustrates the relationship between the measured values

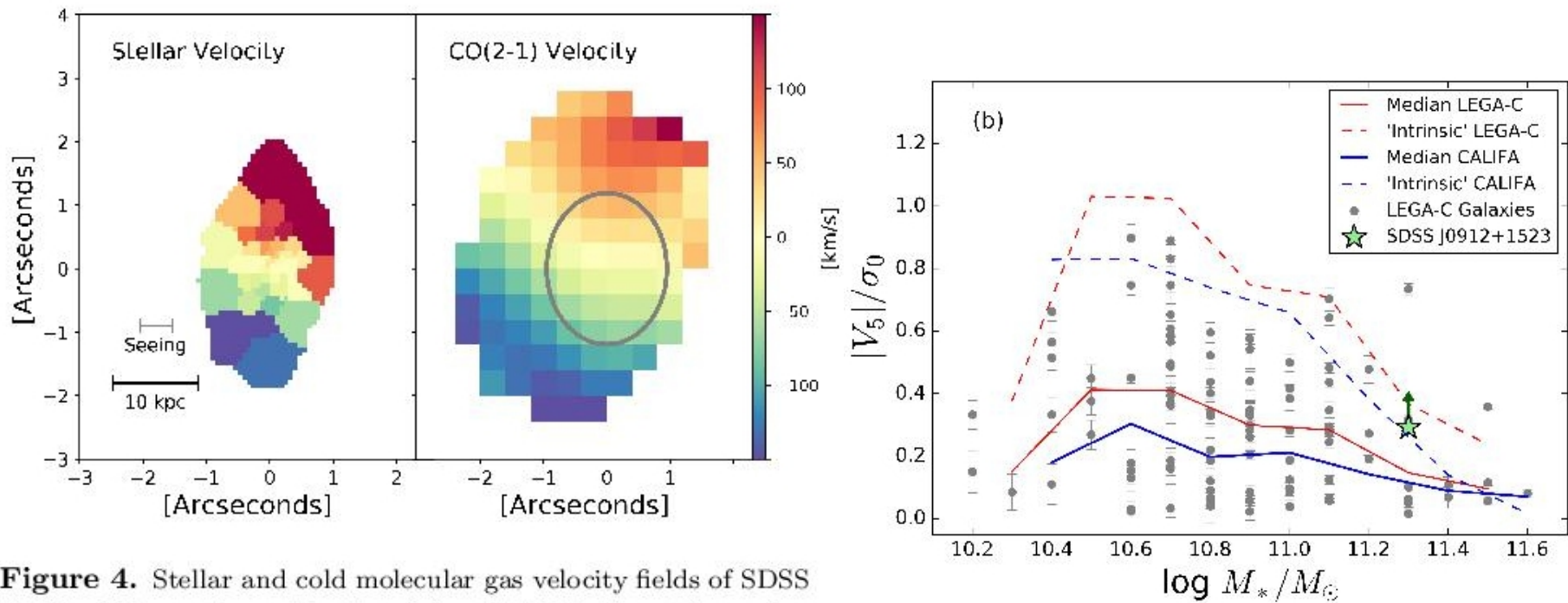# Вращение звезд и CO: в одной плоскости; rotation-dominated?

Figure 4. Stellar and cold molecular gas velocity fields of SDSS J0912+1523, as observed by Gemini and ALMA. The stellar seeing and ALMA beam are indicated in grey. The motion of the cold molecular gas is consistent with the stellar component.